AD-A134 099 POINT-BY-POINT MATRIX EFFECT CALIBRATION FOR THE QUANTITATIVE ANALYSIS OF..(U) CORNELL UNIV ITHACA NY DEPT OF CHEMISTRY A A GALUSKA ET AL. 13 OCT 83 TR-12 1/1

UNCLASSIFIED N00014-80-C-0538 F/G 20/12 NL

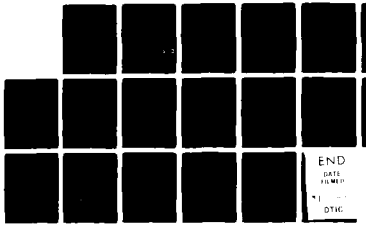

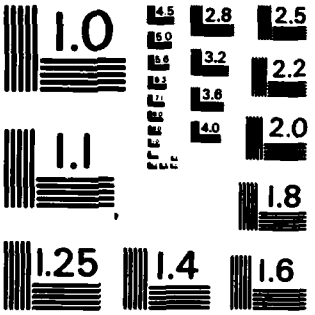

OFFICE OF NAVAL RESEARCH
CONTRACT N0014-80-C-0538
TASK NO. NR 051-736
TECHNICAL REPORT NO. 12

POINT-BY-POINT MATRIX EFFECT CALIBRATION FOR THE QUANTITATIVE ANALYSIS OF LAYERED SEMICONDUCTORS BY SECONDARY ION MASS SPECTROMETRY

A. A. GALUSKA AND G. H. MORRISON*

DEPARTMENT OF CHEMISTRY
CORNELL UNIVERSITY
ITHACA, NEW YORK 14853

PREPARED FOR PUBLICATION
IN
ANALYTICAL CHEMISTRY

OCTOBER 13, 1983

SECURITY CLASSIFICATION OF THIS PAGE (When Data Entered)

REPORT DOCUMENTATION PAGE

READ INSTRUCTIONS BEFORE COMPLETING FORM

1. REPORT NUMBER: Technical Report No. 12	2. GOVT ACCESSION NO.: AD-A134099
3. RECIPIENT'S CATALOG NUMBER:	
4. TITLE (and Subtitle): POINT-BY-POINT MATRIX EFFECT CALIBRATION FOR THE QUANTITATIVE ANALYSIS OF LAYERED SEMICONDUCTORS BY SECONDARY ION MASS SPECTROMETRY	5. TYPE OF REPORT & PERIOD COVERED: Interim Technical Report
	6. PERFORMING ORG. REPORT NUMBER:
7. AUTHOR(s): A.A. Galuska and G.H. Morrison	8. CONTRACT OR GRANT NUMBER(s): N00014-80-C-0538
9. PERFORMING ORGANIZATION NAME AND ADDRESS: Dept. of Chemistry, Cornell University, Ithaca, N.Y. 14853	10. PROGRAM ELEMENT, PROJECT, TASK AREA & WORK UNIT NUMBERS: NR051-736
11. CONTROLLING OFFICE NAME AND ADDRESS: ONR (472), 800 N. Quincy St., Arlington, VA 22217	12. REPORT DATE: October 13, 1983
	13. NUMBER OF PAGES: 28 pages
14. MONITORING AGENCY NAME & ADDRESS(if different from Controlling Office):	15. SECURITY CLASS. (of this report): unclassified
	15a. DECLASSIFICATION/DOWNGRADING SCHEDULE:

16. DISTRIBUTION STATEMENT (of this Report)

Approved for public release: distribution unlimited

17. DISTRIBUTION STATEMENT (of the abstract entered in Block 20, if different from Report)

18. SUPPLEMENTARY NOTES

Prepared for publication in ANALYTICAL CHEMISTRY

19. KEY WORDS (Continue on reverse side if necessary and identify by block number)

Secondary Ion Mass Spectrometry, Ion yield, Sputtering yield, Superlattice and interface calibration, Matrix effects, Molecular beam epitaxy, $Al_xGa_{1-x}As$, Ion implantation, Rutherford backscattering spectrometry

20. ABSTRACT (Continue on reverse side if necessary and identify by block number)

Point-by-point matrix effect calibration is applied to a variety of $Al_xGa_{1-x}As$ multilayer-multimatrix samples grown by molecular beam epitaxy. The procedure uses the linear dependence of secondary ion yields and sputtering yields on matrix composition to quantify depth profiles through matrix gradients and interfaces. The proposed method provides accurate results in the analysis of samples too complex for conventional quantitative analysis by secondary ion mass spectrometry.

DD FORM 1 JAN 73 1473

SECURITY CLASSIFICATION OF THIS PAGE (When Data Entered)

POINT-BY-POINT MATRIX EFFECT CALIBRATION FOR THE QUANTITATIVE ANALYSIS OF LAYERED SEMICONDUCTORS BY SECONDARY ION MASS SPECTROMETRY

A. A. Galuska and G. H. Morrison*

Department of Chemistry
Cornell University
Ithaca, New York 14853

BRIEF

Using the linear dependence of secondary ion yields and sputtering yields on matrix composition, a point-by-point matrix effect calibration is applied to $Al_xGa_{1-x}As$ multilayer-multimatrix samples.

POINT-BY-POINT MATRIX EFFECT CALIBRATION FOR THE QUANTITATIVE ANALYSIS OF LAYERED SEMICONDUCTORS BY SECONDARY ION MASS SPECTROMETRY

A. A. Galuska and G. H. Morrison*

Department of Chemistry
Cornell University
Ithaca, New York 14853

ABSTRACT

Point-by-point matrix effect calibration is applied to a variety of $Al_xGa_{1-x}As$ multilayer-multimatrix samples grown by molecular beam epitaxy. The procedure uses the linear dependence of secondary ion yields and sputtering yields on matrix composition to quantify depth profiles through matrix gradients and interfaces. The proposed method provides accurate results in the analysis of samples too complex for conventional quantitative analysis by secondary ion mass spectrometry.

*Author to whom reprint requests should be addressed.

Secondary ion mass spectrometry (SIMS) is often used to monitor elemental depth distributions in solids and solid interfaces. The technique is highly sensitive for most elements and has good depth resolution. However, the complexity of the sputtering event has made quantitative analysis difficult. Ion implant standards (1-3) have been successfully used to calibrate the depth profiles of trace elements in homogeneous matrices. However, due to the variation of secondary ion yields and sputtering yields with matrix composition, matrix effects, the quantification of SIMS profiles in multimatrix samples remains a problem.

For $Al_xGa_{1-x}As$ and related matrices, it has recently been shown that practical ion yields τ (ions detected/ atoms sputtered) and sputtering yields S (secondary atoms/primary ion) vary linearly with sample composition (4). In addition, highly precise calibration lines were obtained using relative ion yields $R\tau$ and relative sputtering yields RS. These relative values were obtained by normalizing ion yields and sputtering yields from a sample matrix (τ_x and S_x) to those from a standard matrix (τ_0 and S_0) when both measurements were performed under near identical analysis conditions.

$$R\tau = \tau_x/\tau_0 \qquad (1)$$

$$RS = S_x/S_0 \qquad (2)$$

In this investigation, the application of these calibration lines to the analysis of $Al_xGa_{1-x}As$ multilayer-multimatrix samples is examined. These *superlattices*, as shown in Figure 1, are best characterized as a series of homogeneous matrices. A profile correction program (SLIC), which treats each point of a depth profile as a homogeneous matrix, will be presented. SLIC determines the matrix composition at each point of a depth profile and subsequently performs a point-by-point correction of the trace element distributions. The capabilities and limitations of this method will be discussed.

EXPERIMENTAL SECTION

Sample Preparation. The $Al_xGa_{1-x}As$ matrices were grown by molecular beam epitaxy (MBE) on semi-insulating GaAs substrates. The matrix compositions were determined from the MBE growth parameters and verified to an accuracy of better than 10% (5) using Rutherford backscattering spectroscopy (RBS). In some instances dopants were introduced during the growth process while in others, including the standards, ion implantation was used. Prior to implantation samples were cleaned with acetone and methanol.

Instrumentation. The $Al_xGa_{1-x}As$ layers were grown in a VARIAN MBE-360 machine (6). RBS measurements were carried out on a GENERAL IONEX Tandetron Model 4110A. Analyses were performed using a 2.7 Mev

He^+ ion beam with solid state detection at a 170° angle from the incident beam path. Ion implantation was performed using a hot filament ion source and a magnet for mass separation.

SIMS analysis was carried out on a CAMECA IMS-3F ion microanalyzer (7) interfaced to a HEWLETT PACKARD 9845T microcomputer for control and data acquisition. A 1.0 μA O_2^+ primary beam at an energy of 5.5 KeV was rastered over a 300 X 300 μm area. Positive secondary ions were monitored from an image field 60 μm in diameter. Analyses were performed with a residual pressure of 2 X 10^{-8} torr and an energy window of 130 eV. A multiple sample holder was used to simultaneously mount several samples. Depth measurements on the sputtered craters were performed on a TALYSTEP stylus device.

Software. Programs for instrumental control, data analysis, and matrix correction were written in BASIC for the HP 9845T. The program SLIC (superlatttice and interface calibration) was used to correct depth profiles for matrix effects.

SLIC is a comprehensive matrix correction program. For $Al_xGa_{1-x}As$ matrices, the matrix composition and depth at each point of a depth profile is determined by an iterative process involving calibration lines for both relative sputtering yield and the relative ion yield of $^{75}As^+$. Dopant profiles are then corrected for matrix changes using the appropriate dopant calibration lines.

Procedure. Each sample was mounted with three standards, created by ion implantation, using a multiple sample holder. The standards, including in each case GaAs and two different $Al_xGa_{1-x}As$ matrices, and the sample were inserted simultaneously to insure nearly identical analysis conditions. After allowing the pressure in the sample chamber to reach a steady-state condition, the primary beam was focused to a spot of about 100 μm in diameter, and the proper mass settings were determined. Standards and sample were analyzed consecutively without changing any instrumental parameters. Using the depth profiles of the standards, matrix calibration lines were constructed and used to correct the sample depth profiles.

RESULTS AND DISCUSSION

Rτ and RS calibration lines can be used to quantify concentration and depth respectively (4). Using Eq. (3), the concentration of analyte at each point of a depth profile C_p (atoms/cm^3) can be determined.

$$C_p = I_p/R\tau_x \cdot \tau_0 \cdot D_p \cdot A \qquad (3)$$

$R\tau_x$ is the relative sputtering yield determined from a calibration

line for the appropriate value of x, and τ_0 is the practical ion yield of the analyte in the standard matrix (GaAs). I_p (counts) and D_p (cm) are the signal and depth increment associated with a given point of a depth profile.

Similarly, the erosion rate at a given point of a depth profile $\dot{z}_p$ (cm/sec) can be determined using Eq. (4).

$$\dot{z}_p = RS_x \cdot \dot{z}_0 \cdot N_0/N_x \qquad (4)$$

RS_x is the relative sputtering yield determined from a calibration line for the appropriate value of x, and $\dot{z}_0$ (cm/sec) is the erosion rate of the standard matrix (GaAs). N_0 and N_x are the atomic densities of the standard and sample matrix respectively.

With Eqs. (3) and (4) a multilayer-multimatrix sample can now be analyzed. The most critical ingredient of such an analysis is the determination of the matrix structure. The program SLIC exploits the fact that the concentration of As in $Al_xGa_{1-x}As$ matrices is a constant, and that the relative ion yield of $^{75}As^+$ in $Al_xGa_{1-x}As$ matrices can be readily calibrated. If the value of $R\tau_x$ in Eq. (3) is expressed in terms of the equation for the $^{75}As^+$ calibration line ($R\tau_x^{As} = x \cdot M_{R\tau}^{As} + 1$; where $M_{R\tau}^{As}$ is the slope of the line), the equation can be manipulated to the following form:

$$x = \{(I_p^{As}/C_p^{As} \cdot A \cdot \tau_0^{As} \cdot D_p) - 1\}/M_{R\tau}^{As} \qquad (5)$$

Except for D_p, the values for all the variables on the right side of Eq. (5) can be readily determined. Since D_p is directly related to $\dot{z}_p$ ($D_p = \dot{z}_p \cdot T_p$; where T_p is the number of seconds per point), it can be expressed in terms of Eq. (4). If RS_x is replaced with the corresponding equation for the RS calibration line, Eq. (6) is obtained.

$$\begin{aligned} D_p &= (M_{RS} \cdot x + 1) \cdot \dot{z}_0 \cdot N_0/N_x \cdot T_p \\ &= (M_{Rz}^{\circ} \cdot x + 1) \cdot \dot{z}_0 \cdot T_p \end{aligned} \qquad (6)$$

M_{RS} is the slope of the RS calibration line, and M_{Rz}° is the slope of the corresponding relative erosion rate calibration line ($M_{Rz}^{\circ} = M_{RS} \cdot N_x/N_0$). Once again the values of D_p and x are the only unknown quantities.

For each point of a depth profile, the program SLIC determines the matrix structure by performing the following process. It initially assumes that x = 0. The corresponding value of D_p is determined from Eq. (6), and employed in Eq. (5) to obtain a better approximation of x. This process is reiterated until the value of x

converges. In this manner, the matrix structure can be determined despite matrix gradients, interfaces, and plateaus.

Capabilities and Limitations. As shown in Figure 2a, matrix effects can drastically distort SIMS analyses through multilayer-multimatrix samples. This depth profile of a boron implant through a GaAs and a $Al_xGa_{1-x}As$ layer shows a large irregularity at 31 time units. This irregularity is due to the changing matrix effects at the interface. In Figure 2b, SLIC was used to determine the Al distribution and correct the $^{11}B^+$ implant distribution. Upon correction, the implant distribution was transformed into the near gaussian shape which was expected.

The crucial factor influencing the quality of the matrix corrections performed by SLIC is the accuracy with which the matrix structure can be determined. This accuracy can be checked with RBS. RBS analysis is accurate to about 10%, and has an detection limit of 1% for $Al_xGa_{1-x}As$ matrices. In Figure 3, a complex $Al_xGa_{1-x}As$ sample was analyzed by both SIMS and RBS. The Al concentration at specific regions of the superlattice was determined using SLIC and standard RBS techniques (5). As shown in Table I, the values determined by the two techniques agree quite well. In fact, the two sets of data are not statistically different at a 95% confidence level.

In addition to matrix composition, the point-by-point correlation between matrix structure and dopant distribution is critical. Small

differences between the actual and the measured matrix structure can significantly influence the corrections performed on dopant distributions. As apparent in Figure 4, the $^{75}As^{+}$ signal tracts the Al distribution quite well. SLIC uses this correlation to precisely determine matrix structures. However, errors can still result from the correlation between matrix structure and dopant distribution. For example, there is a dead time between the measurement of the matrix signal and the dopant signal for each point of a depth profile. When this dead time is large compared to the abruptness of the matrix changes, the matrix and dopant signals will be obtained from different matrix regions. Consequently, the dopant signal will be calibrated for the wrong matrix composition. Fortunately, this type of error can usually be avoided by minimizing the dead time and reducing the sputtering rate.

Another obstacle to quantitative multilayer-multimatrix analysis concerns molecular interferences. Molecular ions are frequently the source of the high background signals commonly observed during elemental analysis. Molecular signals, like elemental ion yields, can change with matrix composition. When analyzing a multimatrix sample, failure to correct for the changing abundance of interfering molecular ions can lead to erroneous elemental distributions. For example, in Figure 5a, the $^{28}Si^{+}$ profile (dotted line) tracts the Al^{2+} profile (solid line) through the alternating GaAs and $Al_xGa_{1-x}As$ layers even though this region has not been doped with Si. Fortunately, these changing background levels can often be linearly correlated to the

matrix composition, For example, provided the background signals are normalized to erosion rate, a precise background signal calibration line can be obtained for Si in $Al_xGa_{1-x}As$. The background signals can then be subtracted point-by-point prior to quantification. In Figure 5b, both a background corrected (dotted line) and an uncorrected (dashed line) Si concentration depth profile are presented. In the corrected version, nearly all the distortions produced by the changing background levels are removed. The doped region at the surface remains followed by a region with the Si concentratrion below the detection limit (5×10^{17} atom/cm^3) of Si in GaAs.

The full utility of SLIC can be appreciated when very complex samples are analyzed. In Figure 6, SLIC has been used to quantitatively analyze a complex $Al_xGa_{1-x}As$ superlattice grown by MBE with Be and Si dopants. In the uncorrected profile, Figure 6a, both the Be and Si distributions follow the $^{75}As^+$ signal due to the changing matrix effects. Upon calibration, both the Be and Si distributions have changed substantially. As expected from the growth conditions, the Be concentration generally increases as the Al concentration decreases and vice versa. In addition, excluding the surface build up, the Si distribution has generally leveled out at 4×10^{18} atom/cm^3. Without SLIC, this type of analysis could not have been made

In summary, SLIC is a very precise program for applying calibration lines to the problem of matrix effects in complex samples.

Although most of the work to date has been applied to $Al_xGa_{1-x}As$ matrices, this procedure can be used in related matrices, such as $In_xGa_{1-x}As$ and $GaAs_{1-x}Sb_x$. In addition, work in this laboratory indicates that similar methods can be applied to Group III and V compound matrices in which several elements are changing simultaneously.

ACKNOWLEDGMENT

The authors gratefully acknowledge the assistance of C. Palmstrom and J. Mayer with the RBS measurements, and B. Shaft and G. Wicks for the growth of the MBE matrices. Ion implantation was performed at the National Research and Resource Facility for Submicron Structures at Cornell.

CREDIT

This work was supported by the National Science Foundation and the Office of Naval Research.

LITERATURE CITED

(1) Gries, W. H. Int. J. Mass Spectrum. Ion Phys. 1979, 30, 97-112.

(2) Leta, D. P.; Morrison, G. H. Anal. Chem. 1980, 52, 514-519.

(3) Leta, D. P.; Morrison, G. H. Anal. Chem. 1980, 52, 277-280.

(4) Galuska, A. A.; Morrison, G. H. Anal. Chem. submitted 1983.

(5) Mayer, J. W.; Ziegler, J. F.; Chang, L. L.; Tsu, R.; Esaki, L. J. Appl. Phys. 1973, 44, 2322-2325.

(6) Daries, G. J.; Heckingbottom, R.; Ohno, H.; Wood, C. E. C.; Calawa, A. R. Appl. Phys. Lett. 1980, 37, 290-292.

(7) Ruberol, J. M.; Leparoux, M.; Autier, B.; Gourgout, J. M. VIIIth International Congress on X-ray Optics and Microanalysis and 12th Annual Conference of the Microbeam Analysis Society, Boston, MA, 1977, pp 133A-133D.

Table I. Point-by-point Comparison of Al Concentrations Determined by SIMS and RBS Analyses

Point	Al Concentration (X 10^{21} atom/cm^3) RBS	SIMS	Deviation
1	12.0	13.0	-1.0
2	4.2	3.9	+0.3
3	5.1	4.8	+0.3
4	5.1	4.7	+0.4
5	5.2	4.7	+0.5
6	11.0	11.0	0.0
7	1.0	1.3	-0.3
8	4.9	5.7	-0.8

Avg Deviation = -0.075

FIGURE CAPTIONS

Figure 1. A hypothetical $Al_xGa_{1-x}As$ superlattice. The thickness T of the layers can vary from several angstroms to several microns while x can be varied from 0 to 1.

Figure 2. SIMS depth profile of a 250 Kev $^{11}B^+$ implant into a $GaAs/Al_{0.3}Ga_{0.7}As/GaAs$ sample. (a) uncorrected profiles of $^{11}B^+$ (...) and $^{75}As^+$ (——); (b) concentration profiles of B (...) {2.0 X 10^{18} atom/cm^3 full scale, and Al (——) {1.0 X 10^{22} atom/cm^3 full scale}.

Figure 3. SIMS and RBS depth profiles of an $Al_xGa_{1-x}As$ superlattice. (a) an uncorrected $^{75}As^+$ SIMS profile; (b) an RBS profile of the total counts from Ga and As.

Figure 4. An uncorrected SIMS depth profile of $^{75}As^+$ (——) and $^{27}Al^{2+}$ (- - -) in an $Al_xGa_{1-x}As$ superlattice.

Figure 5. SIMS depth profile of an $(GaAs/Al_{0.35}Ga_{0.65}As)n$ superlattice doped in the first 0.4 μm with Si. (a) uncorrected profiles of Al^{2+} (——) and $^{28}Si^+$(...); (b) concentration (atom/cm^3) profiles of Al^{2+} (——), and Si with (...) and without (- - -) background correction.

Figure 6. SIMS depth profile of an $Al_xGa_{1-x}As$ superlattice doped with Be and Si. (a) uncorrected profiles of $^{9}Be^{+}$ (- - -), $^{28}Si^{+}$ (...), and $^{75}As^{+}$ (——); (b) concentration profiles of Be (- - -) {5.0×10^{19} atom/cm^3 full scale}, Si (...) {9.0×10^{19} atom/cm^3 full scale}, and Al (——) {1.5×10^{22} atom/cm^3 full scale}.

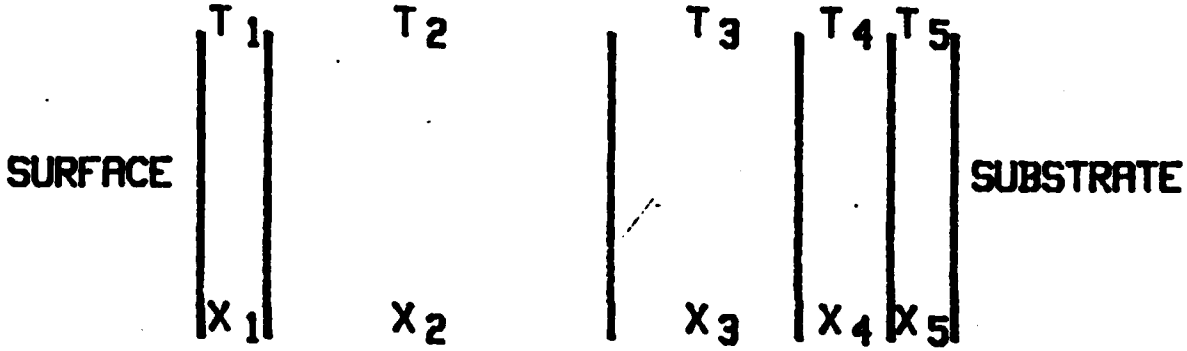
T 1
T 2
T 3
T 4
T 5
SURFACE
SUBSTRATE
X 1
X 2
X 3
X 4
X 5

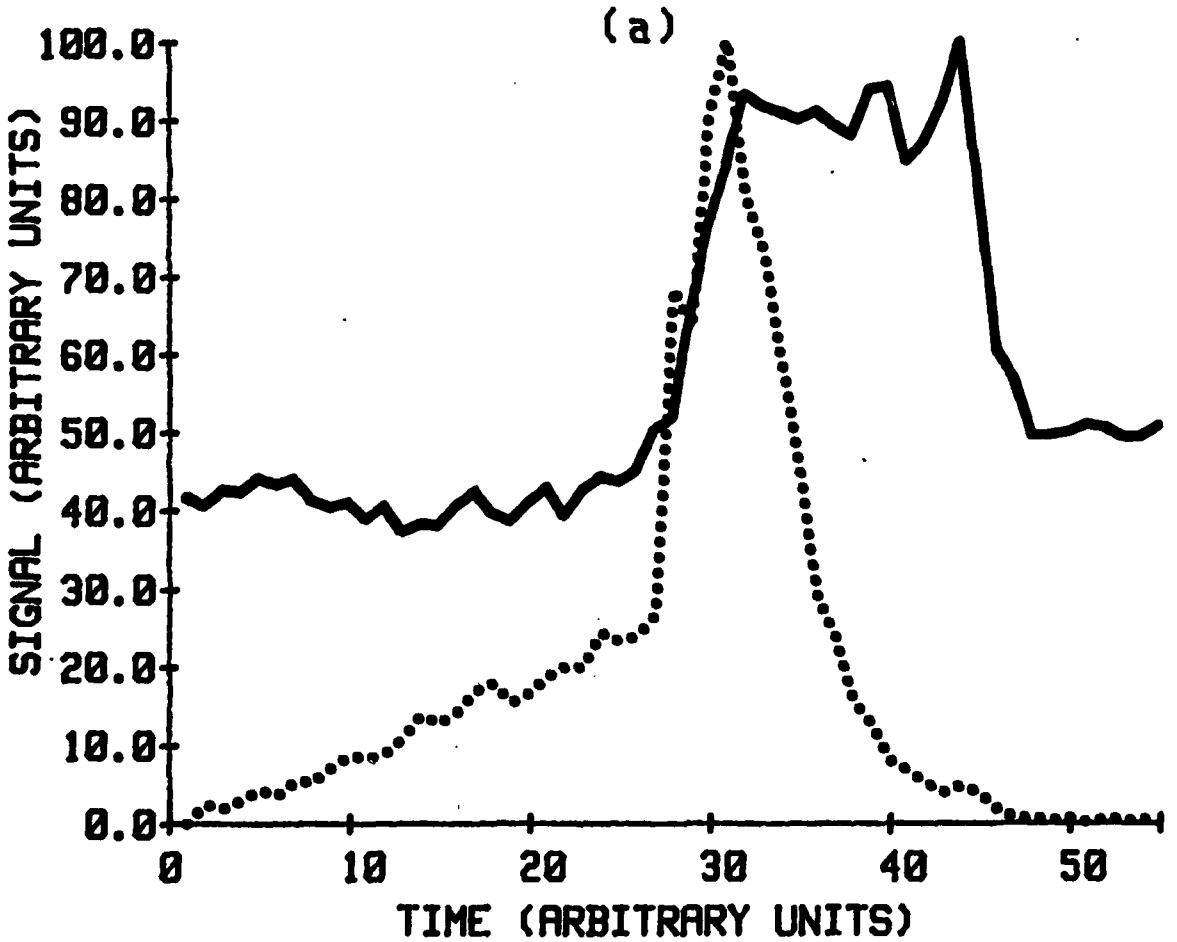
(a)
100.0
90.0
80.0
70.0
60.0
50.0
40.0
30.0
20.0
10.0
0.0
SIGNAL (ARBITRARY UNITS)
0
10
20
30
40
50
TIME (ARBITRARY UNITS)

(b)

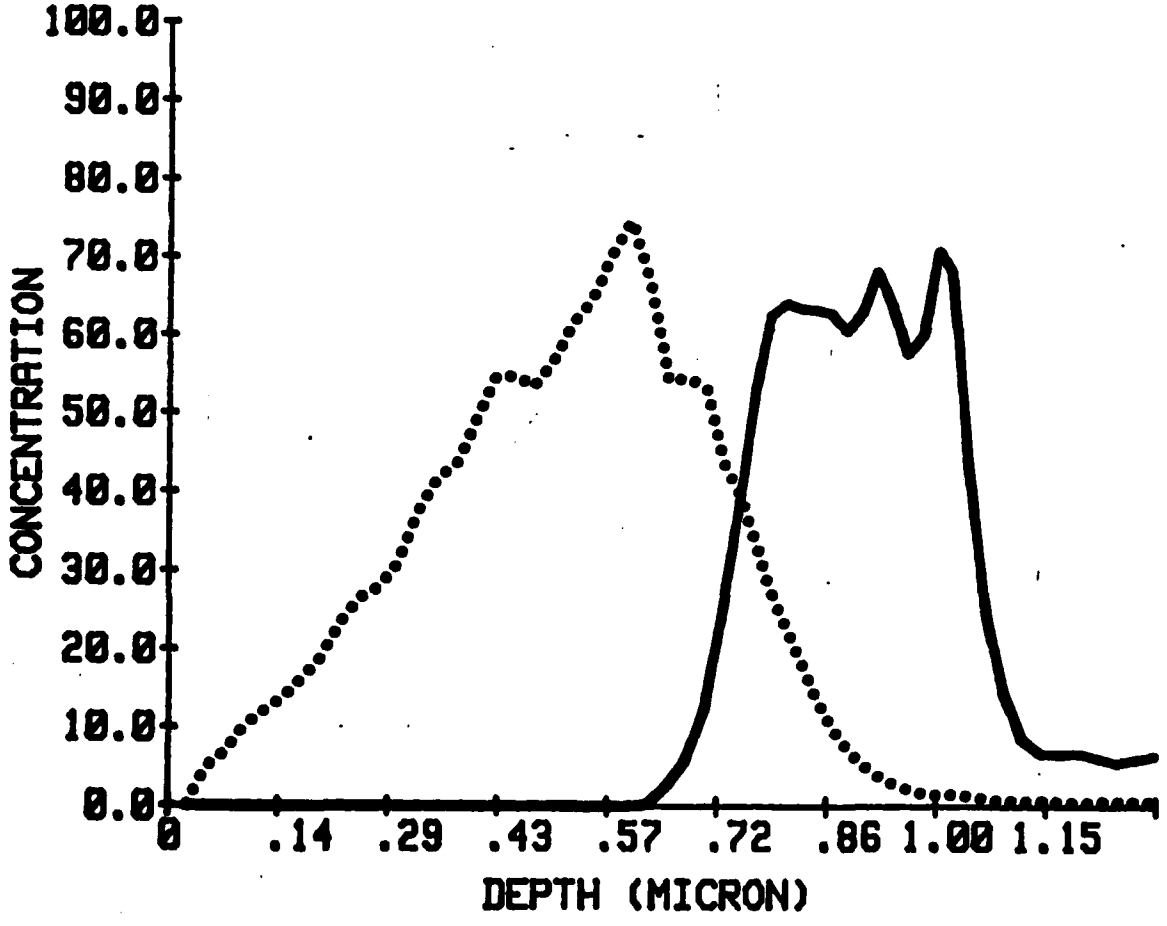
100.0
90.0
80.0
70.0
60.0
50.0
40.0
30.0
20.0
10.0
0.0
CONCENTRATION
0
.14
.29
.43
.57
.72
.86
1.00
1.15
DEPTH (MICRON)

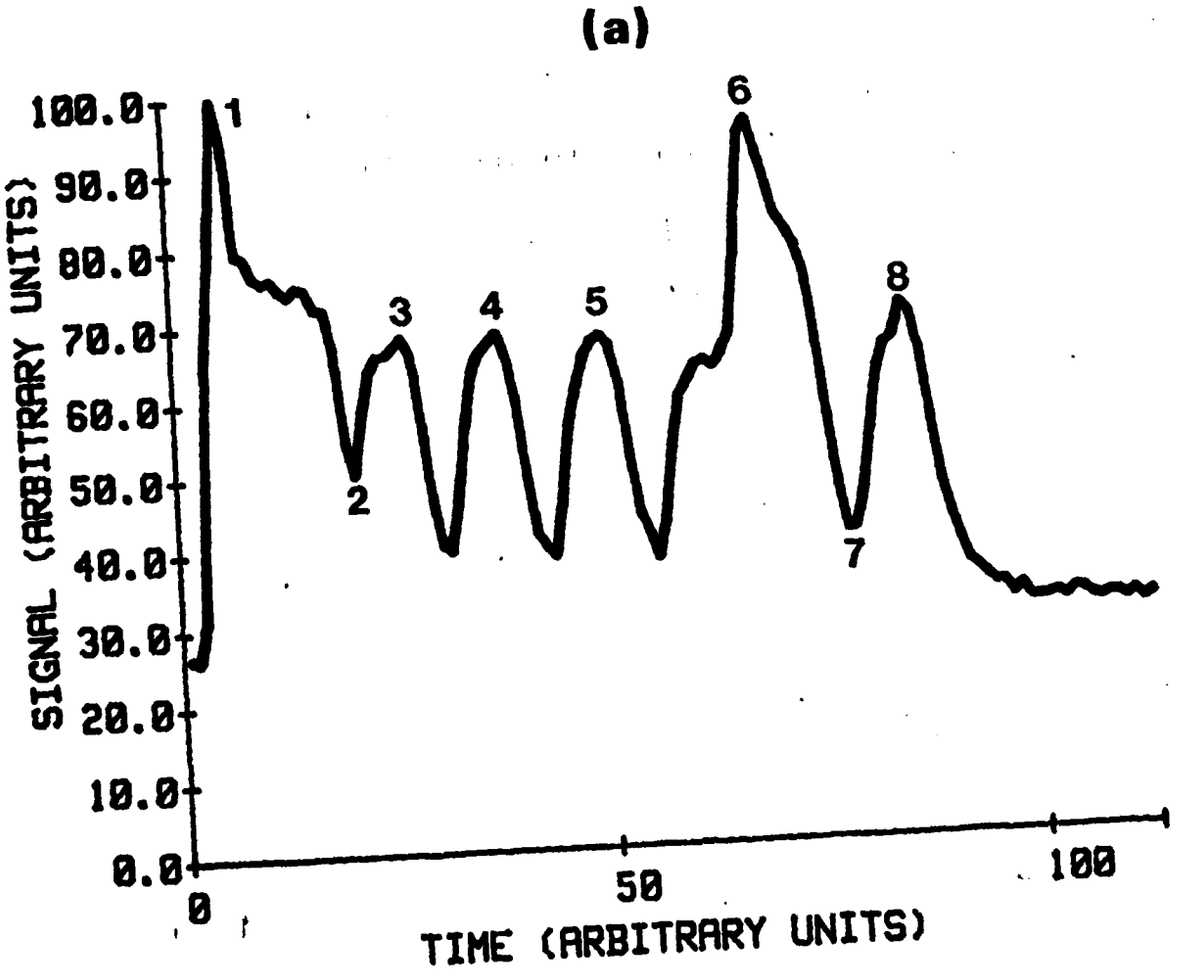
(a)
100.0
90.0
80.0
70.0
60.0
50.0
40.0
30.0
20.0
10.0
0.0
SIGNAL (ARBITRARY UNITS)
1
2
3
4
5
6
7
8
0
50
100
TIME (ARBITRARY UNITS)

(b)

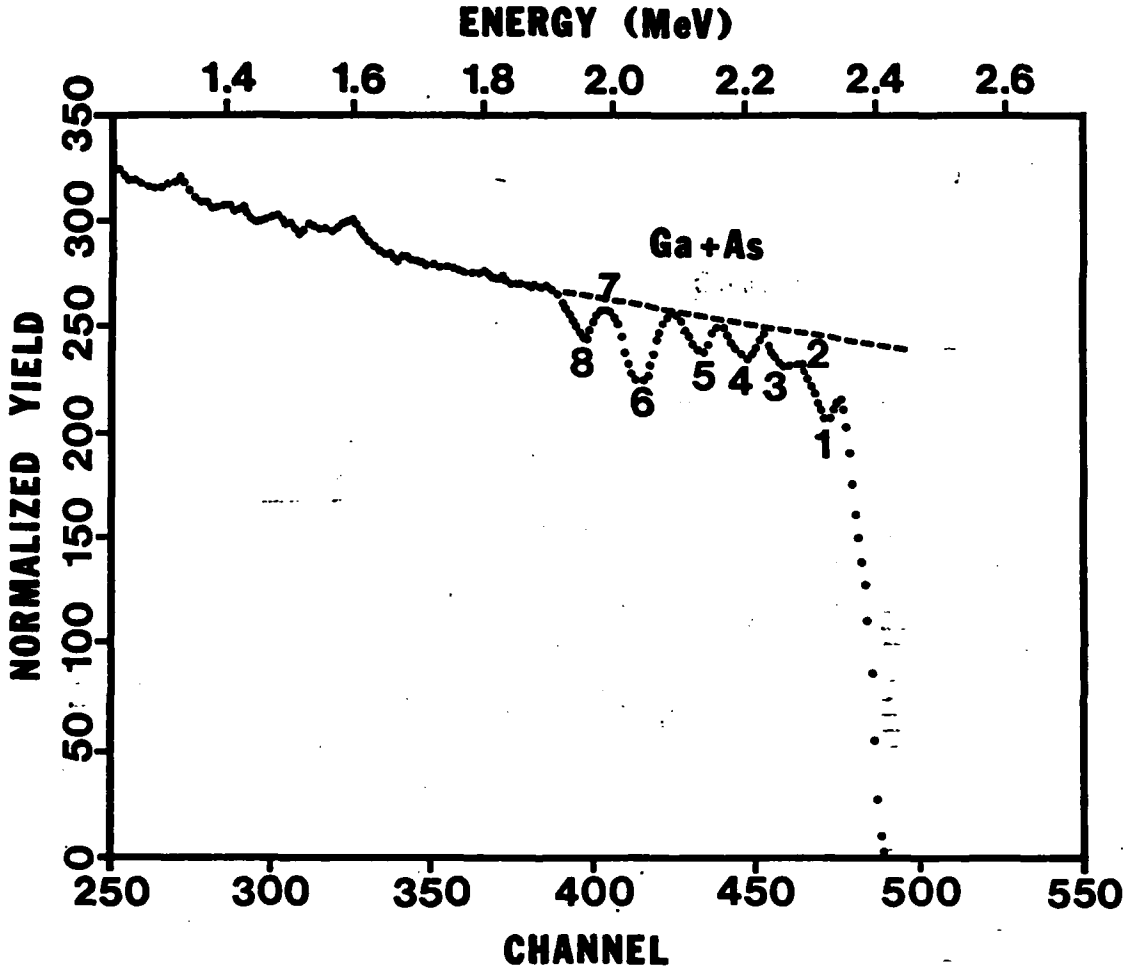
ENERGY (MeV)
1.4
1.6
1.8
2.0
2.2
2.4
2.6
NORMALIZED YIELD
0
50
100
150
200
250
300
350
Ga+As
7
8
6
5
4
3
2
1
250
300
350
400
450
500
550
CHANNEL

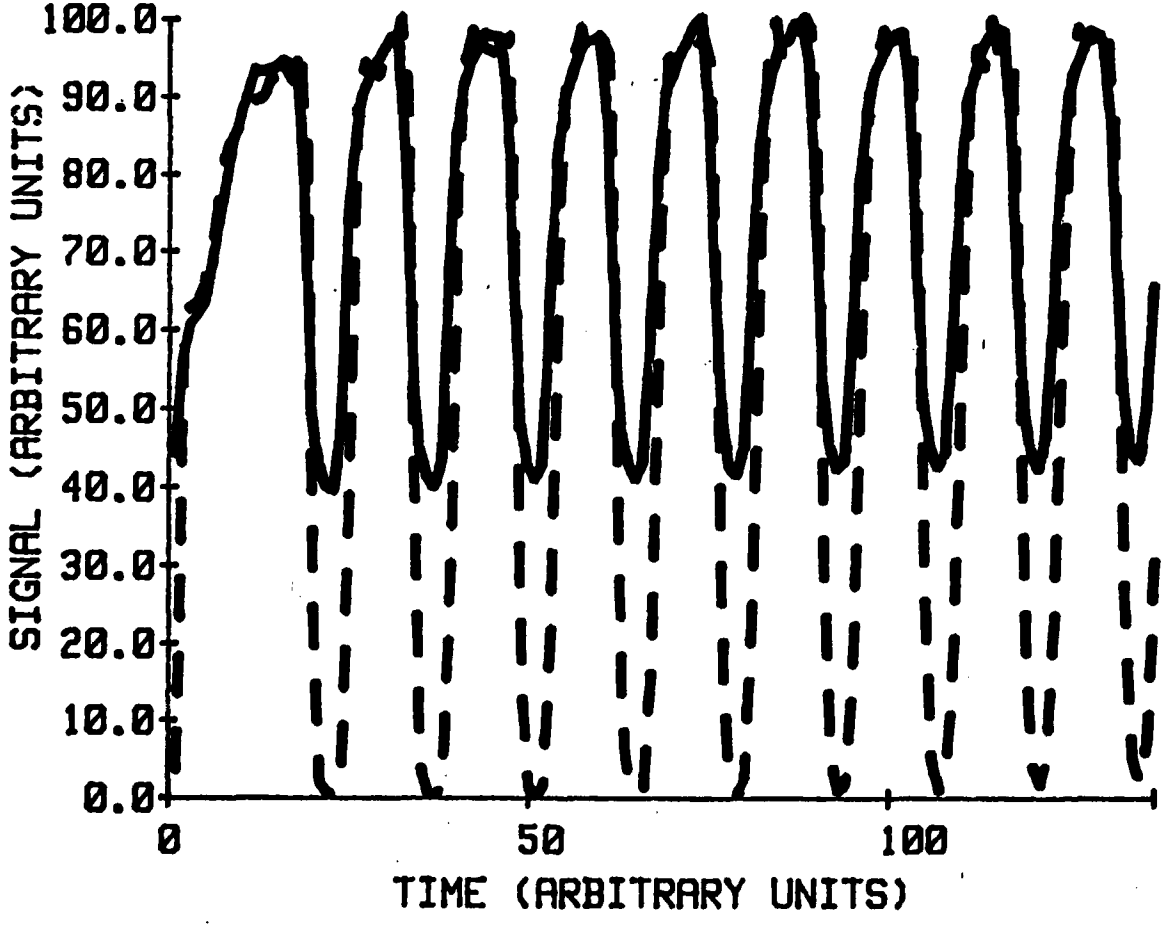
100.0
90.0
80.0
70.0
60.0
50.0
40.0
30.0
20.0
10.0
0.0
SIGNAL (ARBITRARY UNITS)
0
50
100
TIME (ARBITRARY UNITS)

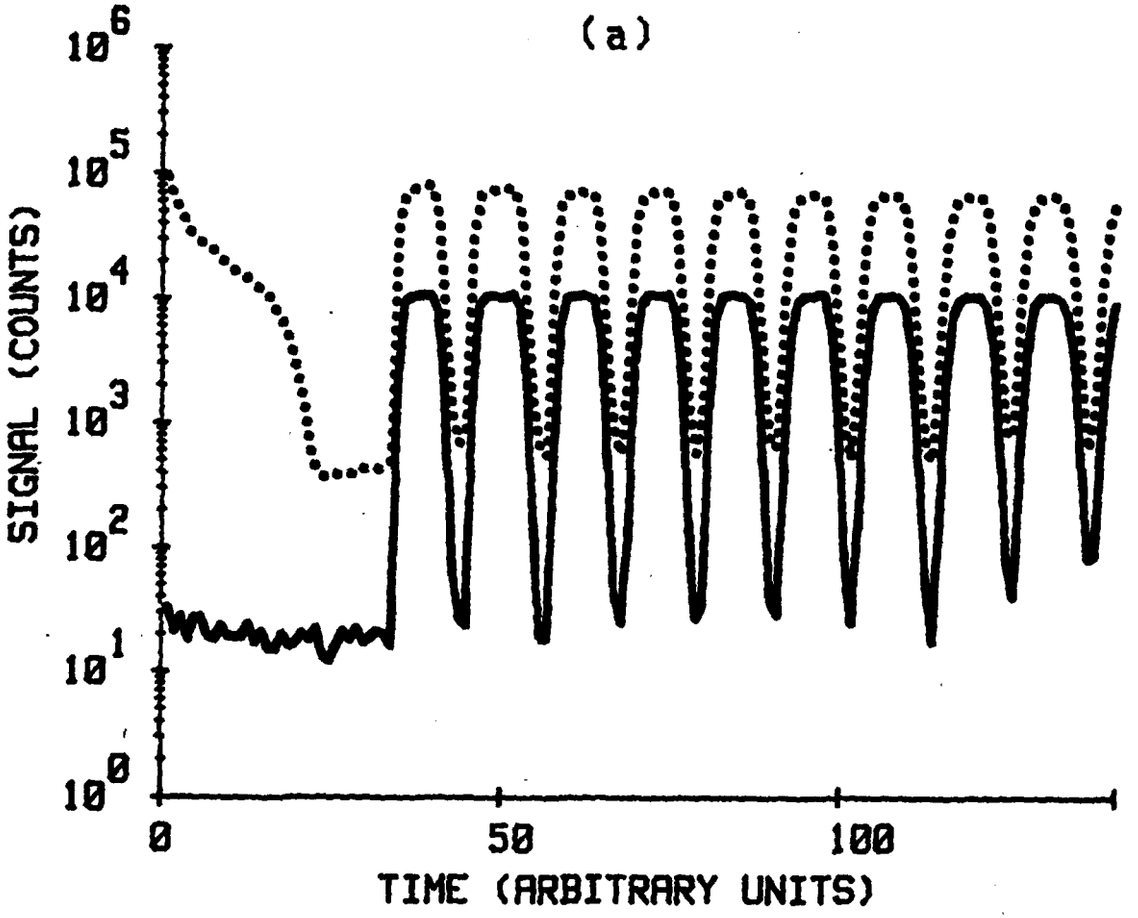
(a)
SIGNAL (COUNTS)
10^6
10^5
10^4
10^3
10^2
10^1
10^0
0
50
100
TIME (ARBITRARY UNITS)

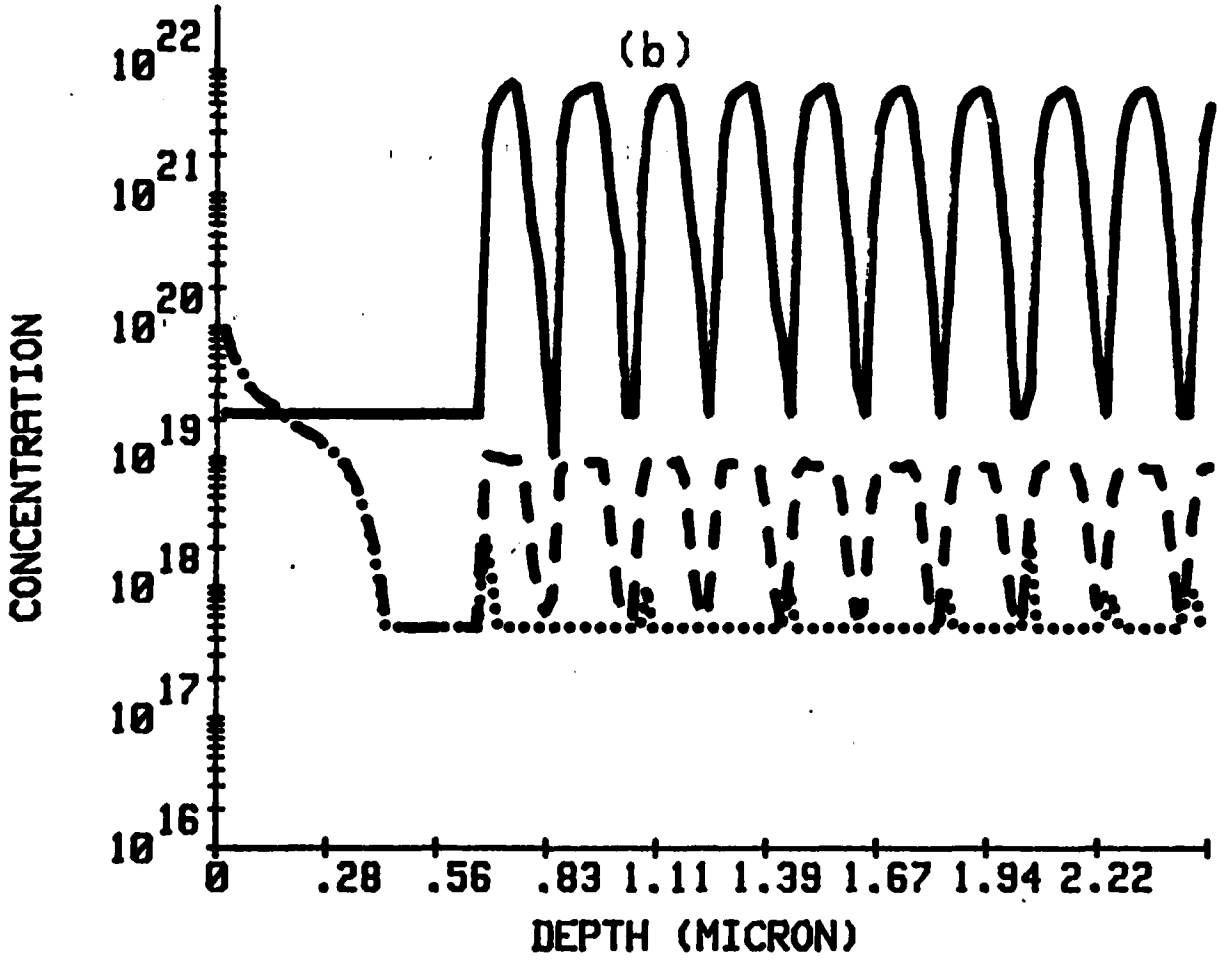
(b)
CONCENTRATION
10^{22}
10^{21}
10^{20}
10^{19}
10^{18}
10^{17}
10^{16}
0
.28
.56
.83
1.11
1.39
1.67
1.94
2.22
DEPTH (MICRON)

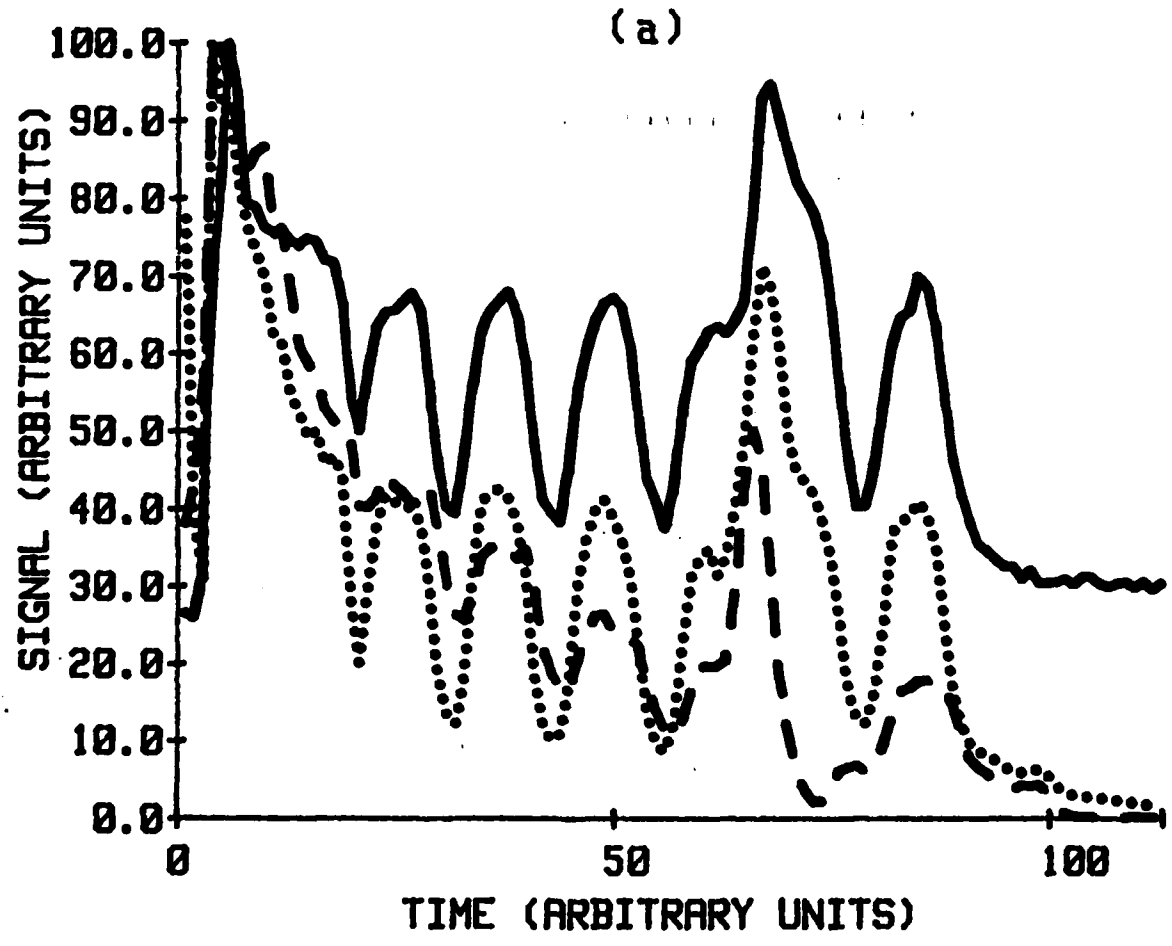
(a)
100.0
90.0
80.0
70.0
60.0
50.0
40.0
30.0
20.0
10.0
0.0
SIGNAL (ARBITRARY UNITS)
0
50
100
TIME (ARBITRARY UNITS)

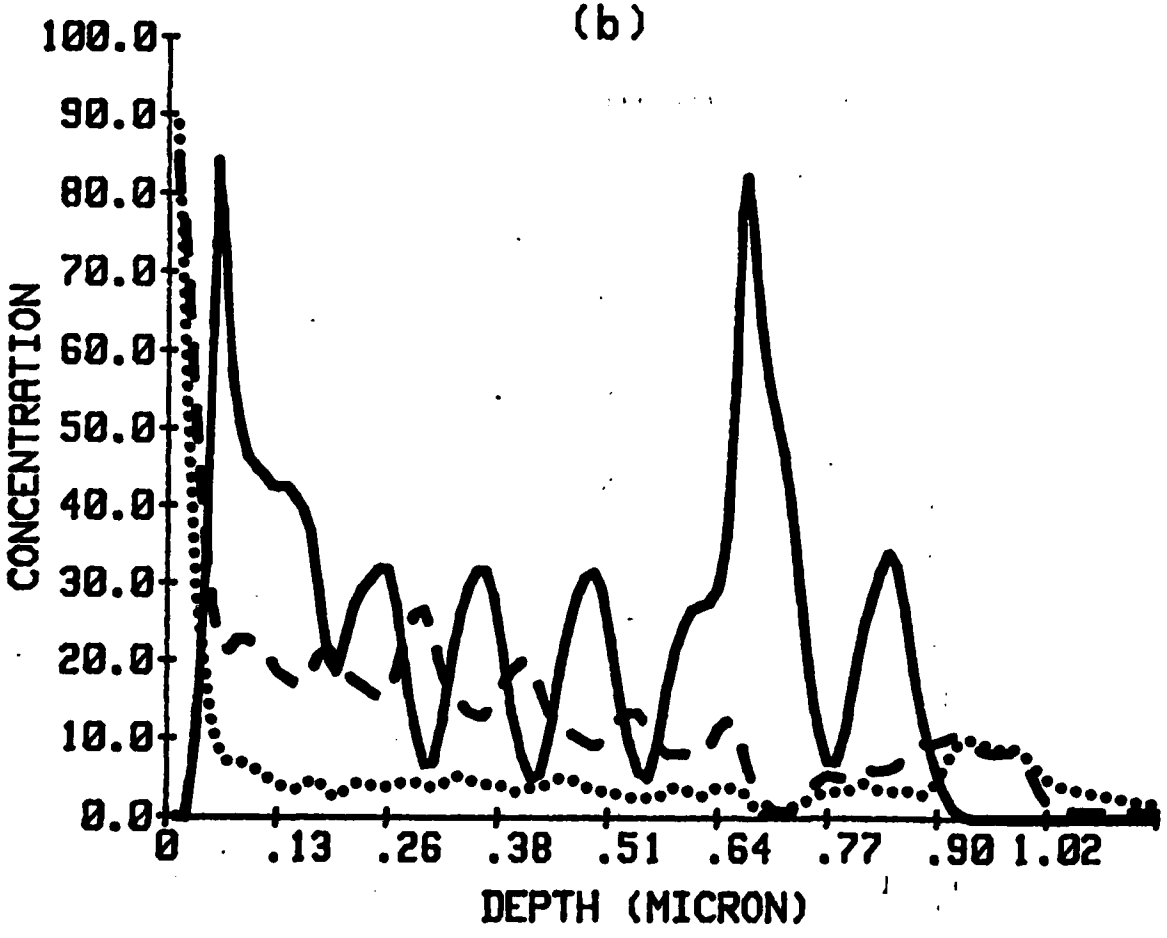
(b)
100.0
90.0
80.0
70.0
60.0
50.0
40.0
30.0
20.0
10.0
0.0
CONCENTRATION
0
.13
.26
.38
.51
.64
.77
.90
1.02
DEPTH (MICRON)

TECHNICAL REPORT DISTRIBUTION LIST, GEN

	No. Copies
Office of Naval Research Attn: Code 472 800 North Quincy Street Arlington, Virginia 22217	2
ONR Branch Office Attn: Dr. George Sandoz 536 S. Clark Street Chicago, Illinois 60605	1
ONR Area Office Attn: Scientific Dept. 715 Broadway New York, New York 10003	1
ONR Western Regional Office 1030 East Green Street Pasadena, California 91106	1
ONR Eastern/Central Regional Office Attn: Dr. L. H. Peebles Building 114, Section D 666 Summer Street Boston, Massachusetts 02210	1
Director, Naval Research Laboratory Attn: Code 6100 Washington, D.C. 20390	1
The Assistant Secretary of the Navy (RE&S) Department of the Navy Room 4E736, Pentagon Washington, D.C. 20350	1
Commander, Naval Air Systems Command Attn: Code 310C (H. Rosenwasser) Department of the Navy Washington, D.C. 20360	1
Defense Technical Information Center Building 5, Cameron Station Alexandria, Virginia 22314	12
Dr. Fred Saalfeld Chemistry Division, Code 6100 Naval Research Laboratory Washington, D.C. 20375	1
Dr. Rudolph J. Marcus Office of Naval Research Scientific Liaison Group - Amer. Embassy A.P.O. San Francisco, CA. 96503	1
U.S. Army Research Office Attn: CRD-AA-IP P.O. Box 1211 Research Triangle Park, N.C. 27709	1
Naval Ocean Systems Center Attn: Mr. Joe McCartney San Diego, California 92152	1
Naval Weapons Center Attn: Dr. A. B. Amster, Chemistry Division China Lake, California 93555	1
Naval Civil Engineering Laboratory Attn: Dr. R. W. Drisko Port Hueneme, California 93401	1
Department of Physics & Chemistry Naval Postgraduate School Monterey, California 93940	1
Dr. A. L. Slafkosky Scientific Advisor Commandant of the Marine Corps (Code RD-1) Washington, D.C. 20380	1
Office of Naval Research Attn: Dr. Richard S. Miller 800 N. Quincy Street Arlington, Virginia 22217	1
Naval Ship Research and Development Center Attn: Dr. G. Bosmajian, Applied Chemistry Division Annapolis, Maryland 21401	1
Naval Ocean Systems Center Attn: Dr. S. Yamamoto, Marine Sciences Division San Diego, California 91232	1
Mr. John Boyle Materials Branch Naval Ship Engineering Center Philadelphia, Pennsylvania 19112	1
Mr. James Kelley DTNSRDC Code 2803 Annapolis, Maryland 21402	1

TECHNICAL REPORT DISTRIBUTION LIST, 051C

	No. Copies
Dr. M. B. Denton Department of Chemistry University of Arizona Tucson, Arizona 85721	1
Dr. R. A. Osteryoung Department of Chemistry State University of New York at Buffalo Buffalo, New York 14214	1
Dr. B. R. Kowalski Department of Chemistry University of Washington Seattle, Washington 98105	1
Dr. S. P. Perone Department of Chemistry Purdue University Lafayette, Indiana 47907	1
Dr. D. L. Venezky Naval Research Laboratory Code 6130 Washington, D.C. 20375	1
Dr. H. Freiser Department of Chemistry University of Arizona Tuscon, Arizona 85721	1
Dr. Fred Saalfeld Naval Research Laboratory Code 6110 Washington, D.C. 20375	1
Dr. H. Chernoff Department of Mathematics Massachusetts Institute of Technology Cambridge, Massachusetts 02139	1
Dr. K. Wilson Department of Chemistry University of California, San Diego La Jolla, California	1
Dr. A. Zirino Naval Undersea Center San Diego, California 92132	1
Dr. John Duffin United States Naval Postgraduate School Monterey, California 93940	1
Dr. G. M. Hieftje Department of Chemistry Indiana University Bloomington, Indiana 47401	1
Dr. Victor L. Rehn Naval Weapons Center Code 3813 China Lake, California 93555	1
Dr. Christie G. Enke Michigan State University Department of Chemistry East Lansing, Michigan 48824	1
Dr. Kent Eisentraut, MBT Air Force Materials Laboratory Wright-Patterson AFB, Ohio 45433	1
Walter G. Cox, Code 3632 Naval Underwater Systems Center Building 148 Newport, Rhode Island 02840	1
Professor Isiah M. Warner Texas A&M University Department of Chemistry College Station, Texas 77840	1
Professor George H. Morrison Cornell University Department of Chemistry Ithaca, New York 14853	1
Professor J. Janata Department of Bioengineering University of Utah Salt Lake City, Utah 84112	1
Dr. Carl Heller Naval Weapons Center China Lake, California 93555	1
Dr. L. Jarvis Code 6100 Naval Research Laboratory Washington, D. C. 20375	1

END

DATE
FILMED

11 — 83

DTIC